Journal of
Marine Science and Engineering

MDPI

Article

Enhanced Multi-Objective Evolutionary Algorithm for Green Scheduling of Heterogeneous Quay Cranes Considering Cooperative Movement and Safety

Lingchong Zhong [1,2], Lijun He [1,2,*], Yongcui Li [3], Yu Zhang [1,2], Yong Zhou [1,2] and Wenfeng Li [1,2]

[1] State Key Laboratory of Maritime Technology and Safety, Wuhan University of Technology, Wuhan 430063, China; zhonglc@whut.edu.cn (L.Z.); sanli@whut.edu.cn (Y.Z.); houyong@whut.edu.cn (Y.Z.); liwf@whut.edu.cn (W.L.)
[2] School of Transportation and Logistics Engineering, Wuhan University of Technology, Wuhan 430063, China
[3] Qingdao New Qianwan Container Terminal Co., Ltd., Hanjiang Road, Huangdao District, Qingdao 266000, China; li.yc@qqctn.com.cn
* Correspondence: helj@whut.edu.cn

Abstract: Heterogeneous quay cranes (HQCs) are the main energy-consuming equipment of automated container terminals, and they need to move from one bay to another along the rail and maintain a safe distance from one another. Improving the operational efficiency of HQCs and reducing the ineffective walking distance of HQCs are key to reducing the energy consumption of QCs. In this paper, an energy-efficient HQC cooperative scheduling problem is studied, and the HQCs are required to ensure safe and efficient operation. A multi-objective scheduling model is formulated to minimize the maximum completion time of containers, the average completion time of HQCs, and the total energy consumption of HQCs simultaneously. An Enhanced Multi-Objective Evolutionary Algorithm (EMOEA) is designed to solve this problem using a problem-feature-based encoding method to encode and initialize the population, a cooperative strategy to ensure the safe operating distance of HQCs, and a novel multi-objective evaluation mechanism with effective evolutionary operators. The results indicate that the different operational capacities of HQCs had a significant impact on the three studied objectives, especially for some large-scale problems, and that our algorithm outperforms three other well-known multi-objective algorithms in solving the EHQCCSP.

Keywords: energy efficiency; heterogeneous quay crane scheduling; multi-objective optimization; evolutionary algorithm

check for updates

Citation: Zhong, L.; He, L.; Li, Y.; Zhang, Y.; Zhou, Y.; Li, W. Enhanced Multi-Objective Evolutionary Algorithm for Green Scheduling of Heterogeneous Quay Cranes Considering Cooperative Movement and Safety. *J. Mar. Sci. Eng.* **2023**, *11*, 1884. https://doi.org/10.3390/jmse11101884

Academic Editor: Mihalis Golias

Received: 10 September 2023
Revised: 24 September 2023
Accepted: 25 September 2023
Published: 28 September 2023

1. Introduction

Due to the substantial quantity of large handling equipment, container terminals play a crucial role in energy consumption and pollutant emissions across the entire container transportation network. Consequently, operators of container terminals are under pressure to prioritize energy efficiency and emission reduction. While striving to minimize energy usage is essential, it should not come at the cost of compromising service quality. Every container terminal must explore suitable strategies for energy efficiency without diminishing throughput or hindering service levels. Moreover, with the global economic crisis, the competition among container terminals is intensifying. As container vessel sizes continue to increase, the rapid handling of containers for mega vessels is paramount. Consequently, container terminals need to reduce the vessel turnaround time, a crucial factor in enhancing their service level. However, due to the high cost of handling equipment and limited land resources, expanding equipment or territory is often not feasible. Hence, the efficient and effective scheduling of handling equipment is crucial to elevating the service level of container terminals.

Quay cranes (QCs) are a class of important equipment in automated container terminals that provide container loading and unloading operations for a vessel [1]. Meanwhile, a QC is an expensive kind of equipment because of its high running and maintenance costs and energy consumption [2]. The QC scheduling problem (QCSP) is an important seaside operational planning problem with heterogeneous parallel machine characteristics in an automated container terminal [3–7]. It is very important to obtain a good QC scheduling plan that completes the loading and unloading operations with less time, high energy efficiency, and safety.

With the environmental pollution issue, green operation with energy efficiency has become a pursued objective in modern green ports [8]. In container ports, the QC is the main equipment with the highest power consumption. Generally, the rated power of each QC is more than 2000 KW. Reducing the energy consumption of QCs will play a positive role in the future development of automated container terminals [9]. Therefore, it is of great significance to consider the energy consumption of QCs in the QCSP. However, some previous studies only focused on the optimization of operational efficiency and overlooked the energy consumption of QCs [10]. It should be noted that a scheduling plan for the QCSP with good efficiency may cause more energy consumption in reality [11]. A satisfactory QC scheduling plan should be able to achieve the trade-off between efficiency and energy consumption.

On the other hand, multiple QCs have to move along a common rail for handling containers at different bays simultaneously without conflicts in an automated container terminal. In general, these QCs need to work cooperatively to ensure non-crossing interference and maintain a realistic safety distance. Waiting will inevitably occur due to interference and will waste a substantial amount of time and energy. Nevertheless, conventional QC scheduling methods focus solely on enhancing terminal efficiency without addressing energy conservation. Thus, it is crucial to explore an effective HQC scheduling approach that balances operational efficiency, the HQC workload, and energy consumption. Therefore, when scheduling multiple QCs cooperatively, it is very important to optimize operational efficiency and energy consumption. Nevertheless, most of the studies on the QCSP did not strictly enforce the conflict-free constraint or keep a realistic safety distance between QCs. There are no energy-efficient QCSP studies considering the cooperation of multiple QCs.

Researchers have developed various effective methods to handle the QCSP, such as Zhang et al. [12]. Nevertheless, most of the relevant studies have overlooked the QC movement time on the rail and the no-load operation time. The setups for movement and no-load operation are commonly seen in practical automated container terminals. Additionally, it is often assumed that the QCs are homogeneous in the current QCSP, which means that the operating time of each QC for a container is the same. In practice, heterogeneous QCs (HQCs) are commonly used in real automated container terminals [13]. The operational capacities of the HQCs are different due to their heterogeneous nature. Thus, the handling time for a container (or a bay) on different HQCs is different, which will affect the scheduling plan for the QCSP.

Given the above, it is of great significance to study an energy-efficient heterogeneous quay crane cooperative scheduling problem (EHQCCSP). The difficulties of the EHQCCSP include (1) how to deal with the complex cooperative operational constraints between multiple HQCs considering their movement constraints; (2) how to construct a multi-objective mathematical model with the energy consumption of multiple HQCs; and (3) how to design an effective multi-objective scheduling method to achieve the trade-off between efficiency and energy objectives.

In recent years, evolutionary algorithms (EAs) have been widely used to solve various multi-objective problems [14–16]. These multi-objective EAs (MOEAs) can be roughly divided into two categories according to the fitness evaluation mechanism (FEM). The first is the scalar-based MOEA, which uses a scalar aggregation function [15]. The second is based on non-dominated sorting [14]. However, the first method is unable to fairly divide weights for each objective, and the second method consumes a lot of CPU computing time for large-scale optimization problems. Most importantly, decision makers often need one desired solution for a real-world engineering optimization problem. Thus, selecting a desired solution from the final set of solutions is difficult [17]. To date, studies that use MOEAs to address the EHQCCSP are very limited. There is much room to develop a more efficient MOEA for solving the EHQCCSP.

In this work, we focus on the EHQCCSP. The aim of our work is to design an effective multi-objective scheduling method for the EHQCCSP. The main contributions of this work are summarized as follows:

(1) A new multi-objective model is formulated for the EHQCCSP to minimize the completion time of containers, the average completion time of HQCs, and the total energy consumption of HQCs. Meanwhile, it maintains operational safety.
(2) An enhanced MOEA (EMOEA) is proposed to tackle the EHQCCSP. Effective operators, such as problem-based encoding/decoding and evolutionary operators, are designed to adapt to the EHQCCSP.

The structure of this paper is as follows. Section 2 presents a literature review of previous work. In Section 3, a multi-objective mathematical model for the EHQCCSP is presented. Section 4 describes the proposed EMOEA algorithm. Section 5 gives the experimental study and comparison results. Finally, the conclusions and a discussion of future work are presented in Section 6.

2. Related Work

Our focus in this section is three-fold. First, the previous work on the general QCSP is presented. Second, a brief review is provided on scheduling considering energy consumption in the container terminal. Third, research gaps are given according to the literature review.

In Table 1, we present parts of the literature referenced. The problem classification for QC scheduling is represented as Crane Type | Interference | Objective. The Crane Type specifies the type of QCs as homogeneous or heterogeneous. The Interference field indicates the restrictions of the QCs as non-crossing (cross) and safety margins (safe), while the Objective field denotes performance metrics such as the task completion time ($compl$), the total QC finish time ($finish$), the total QC emission ($emission$), and the vessel delay time ($delay$).

Table 1. Overview of QCSP formulations.

Problem Classification	Reference	Method
Homogeneous/$w_1 \sum finish + w_2 \sum energy$	Tian et al. (2021) [2]	CPLEX
Two different speeds QCs/cross, safe/max($compl$)	Zhang et al. (2017) [12]	AA
Homogeneous/cross, safe/$w_1$max($compl$) + $w_2 \sum finish$	Kaveshgar et al. (2012) [18]	GA
Homogeneous/cross, safe/$w_1$max($compl$) + $w_2 \sum finish$	Kaveshgar et al. (2012) [19]	GA
Homogeneous/cross, safe/$w_1$max($compl$) + $w_2 \sum finish$	Izquierdo et al. (2011) [20]	EDA
Homogeneous/$w_1$max($compl$) + $w_2 \sum delay$	Daganzo et al. (1989) [21]	AA and EA
Homogeneous/cross, safe/max($compl$)	Sun et al. (2019) [22]	EA
Homogeneous/max($compl$)	Huang et al. (2018) [23]	DP
Homogeneous/cross, safe/$w_1$max($compl$) + $w_2 \sum finish$	Castilla et al. (2020) [24]	SIM
Homogeneous/cross, safe/max($compl$)	Dik et al. (2017) [25]	TS
Heterogeneous/max($compl$)	Zhen et al. (2018) [26]	PSO
Homogeneous/cross, safe//$\sum finish$	Wu et al. (2017) [27]	B&B and GA
Homogeneous/cross, safe//$w_1$max($compl$) + $w_2 \sum delay$	He et al. (2015) [28]	PSO and GA
Homogeneous/safe/$w_1 \sum energy + w_2 \sum emission$	Hu et al. (2014) [29]	Rule
Homogeneous/cross/max($compl$)	Diabat et al. (2014) [30]	GA
Homogeneous/$w_1 \sum energy + w_2 \sum delay$	He et al. (2016) [31]	SAO

GA, genetic algorithm; EDA, Estimation-of-Distribution Algorithm; SIM, simulation; AA, approximation algorithm; EA, exact algorithm; DP, dynamic programming; TS, tabu search; PSO, particle swarm optimization; B&B, branch-and-bound method; SAO, Simulation and Optimization.

2.1. The General QCSP

The general QCSP considers a set of containers to be unloaded or loaded at a single vessel and a set of assigned QCs. A lot of studies have been carried out on the general QCSP. Kaveshgar focused on the makespan and the total QC handling time by using a GA [18,19]. Izquierdo et al. [20] used an EDA to address these objectives based on a weighted sum. Zhang et al. [12] studied the QCSP to minimize the makespan and designed an effective approximation algorithm to solve this problem. Daganzo et al. [21] first studied a QCSP and proposed a mixed-integer programming (MIP) model to minimize all ships' aggregate cost of a delay. Sun et al. [22] designed a simple method to deal with non-crossing and movement constraints and proposed an exact method based on Benders decomposition for the QCSP. Huang et al. [23] developed a bounded two-level dynamic programming algorithm for the QCSP in container terminals. Castilla et al. [24] developed a QCSP model to minimize the makespan and the total operation time of QCs. They used a weighted-sum approach to aggregate the two objectives. Dik et al. [25] proposed an algorithm based on the tabu search framework for the QCSP. Zhen et al. [26] presented a QCSP model and developed a particle swarm optimization algorithm to minimize the makespan. To optimize the QCSP with draft and trim constraints, Wu and Ma constructed a MIP model, which aimed to minimize the makespan and the total operation time of QCs. A GA based on a weighted-sum approach was employed to optimize the QCSP [27].

2.2. Scheduling Considering Energy Consumption in Container Terminal

In recent years, optimizing energy consumption in a container terminal has received increasing attention from scholars. Tian et al. [2] constructed a bi-objective QCSP model, including the energy consumption of QCs and the makespan. An exact algorithm with a weighted sum was proposed to solve this model. Nevertheless, they did not consider the practical features of the problem, such as conflict-free movement. He et al. [28] minimized the total transportation energy consumption of all tasks and the total departure delay of all vessels simultaneously for an integrated QC scheduling, internal truck scheduling, and yard crane scheduling problem. The weighted-sum approach was adopted in their proposed algorithm to aggregate the two objectives. Hu et al. [29] applied a novel nonlinear multi-objective mixed-integer programming model that considered a vessel's fuel consumption and emissions for the berth and quay crane allocation problem. Diabat et al. [30] studied the QC assignment and scheduling problem and designed a GA to solve it. He et al. [31] formulated integrated berth allocation and QC assignment as a mixed-integer programming model in order to minimize the total handling energy consumption of all vessels by QCs. Xin et al. [32] investigated the cooperative scheduling problem of QCs and lift-automated guided vehicles considering the energy efficiency. A customized GA with lexicographic and weighted-sum strategies was developed to solve the studied problem.

2.3. Research Gaps

(1) Most of the previous studies on the general QCSP overlooked the setup time, such as the QC movement time on the rail and the no-load operation time. Previous studies assumed that the QCs are homogeneous. However, in practice, HQCs are commonly seen in real automated container terminals. It would be conducive to the optimization of realistic scheduling objectives to consider HQCs in real-world automated container terminals.

(2) There have been several studies on energy-efficient scheduling in container terminals. In reality, multiple QCs (or HQCs) often need to operate cooperatively in an automated container terminal. It is important to conduct a cooperative scheduling study that considers the energy consumption of multiple HQCs.

(3) Almost all of the studies on energy-efficient scheduling in container terminals adopted meta-heuristics with weighted-sum and non-dominated sorting. These multi-objective optimization approaches output a set that contains several solutions. It is very difficult for decision makers to select a preferable solution from the final solution set.

Based on the above gaps, this work focuses on cooperative scheduling considering energy efficiency by taking the energy consumption of multiple HQCs into account, which better meets practical requirements in modern automated container terminals. We constructed a multi-objective model for the studied problem and developed a novel EMOEA to solve the model.

3. Problem Definition and Mathematical Modeling

3.1. Problem Description

As shown in Figure 1, the EHQCCSP can be described as follows. The container vessel is divided into multiple contiguous bays, each of which has a stack of containers. All HQCs are mounted on the same rail parallel to the vessel so that the HQCs cannot cross over each other. At the beginning, an HQC should move from its initial position on the rail to the position of a specified bay and then start to unload the containers on the bay. Containers in the same bay can only be operated by one HQC. After completing one bay task, the HQC moves to the next bay and starts its unloading task. To prevent a collision, cooperative operation is required for two adjacent HQCs to maintain a safety margin (clearance) distance. This clearance is usually measured by the number of bays, which must separate two adjacent HQCs. The movement of HQCs is very slow because they are made of heavy steel [17]. When one container in a bay is unloaded by an HQC, two necessary processes are involved, i.e., the no-load and heavy-load operating processes.

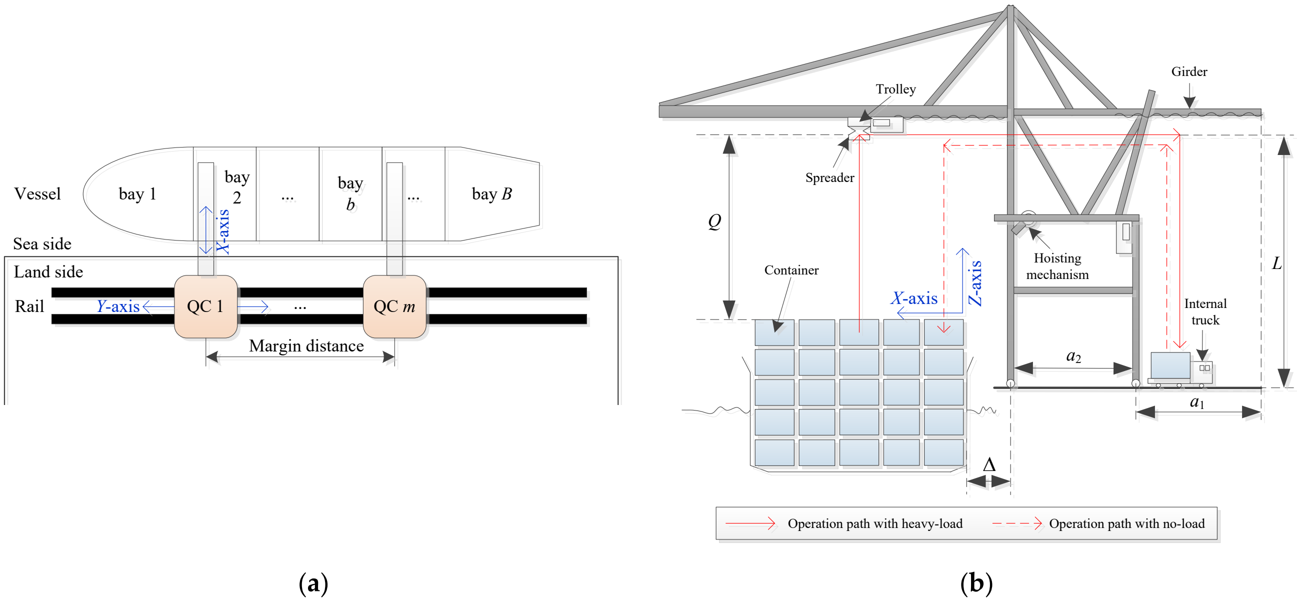

Figure 1. Cooperative operation of HQCs in a container terminal. (**a**) Vertical view of cooperative operation of HQCs; (**b**) lateral view of cooperative operation of an HQC.

In the no-load operating process, the hoisting mechanism (HM) of an HQC lifts its spreader from the initial position to the highest position along the Z-axis. Then, the trolley moves the spreader directly above a container along the X-axis. Finally, the HM lowers the spreader to the position of a container along the Z-axis, and the spreader starts to grab the container for the unloading process.

In terms of the heavy-load operating process, the HM lifts the container from the bay to the highest position along the Z-axis. With the trolley, the container is moved directly above the internal truck along the X-axis. At last, the HM lowers the container to the internal truck along the Z-axis, and the spreader starts to unlock the container. After a container is unloaded, the HQC starts to operate another container in the bay.

The above three processes consume a lot of time and energy. The moving speeds of HQCs on the rail, the moving speeds of the HQCs' trolleys, and the lifting and lowering speeds of the HQCs' HMs are different due to the heterogeneous nature of HQCs. This means that the required time and energy consumption for the three processes are not the same for all HQCs. While an HQC handles a bay task, the container operation sequence will not affect the operation time and energy consumption.

The EHQCCSP involves two coupled sub-problems: (1) divide the bays and allocate them to the given HQCs and (2) arrange the bays for each HQC. We do not need to determine the container sequence in a bay because it has no effect on the operation time and energy consumption. We optimize three objectives simultaneously, i.e., the maximum completion time of containers (C_{max}), the average completion time of HQCs (ATQ), and the energy consumption of HQCs (ECQ). Some relevant assumptions are as follows:

1. All HQCs, containers, and bays are instantaneously available at time zero.
2. Once started, an HQC will not stop its operation on a bay until it completes all containers in the bay.
3. A container can only be unloaded by one HQC at a time, and an HQC can only unload one container at a time.
4. Vessel bays and HQCs are numbered starting from 1 and from the left end of the vessel.
5. Breakdowns are not considered during the operation of HQCs.
6. The trolley and HM move at a constant speed in the no/heavy-load state; acceleration at the beginning and deceleration at the end are not considered.
7. The HQCs move at a constant speed on the rail; acceleration at the beginning and deceleration at the end are not considered.

As shown in Figure 2, the EHQCCSP is similar to the classic non-identical parallel machine scheduling problem in a manufacturing system. The containers are equivalent to jobs, and the HQCs are equivalent to non-identical parallel machines in the workshop. As shown in Figure 1a,b, the differences between the EHQCCSP and the classic non-identical parallel machine scheduling problem lie in the fact that:

(1) The HQCs in the EHQCCSP are mobile. Coordination is required between two adjacent HQCs to maintain a safe distance, while the non-identical parallel machines in the workshop are fixed.
(2) In the EHQCCSP, some setup operations are required for HQCs when unloading containers, such as no-load movements of the trolley and HM. However, the setup operations are generally ignored in a classic non-identical parallel machine scheduling problem.

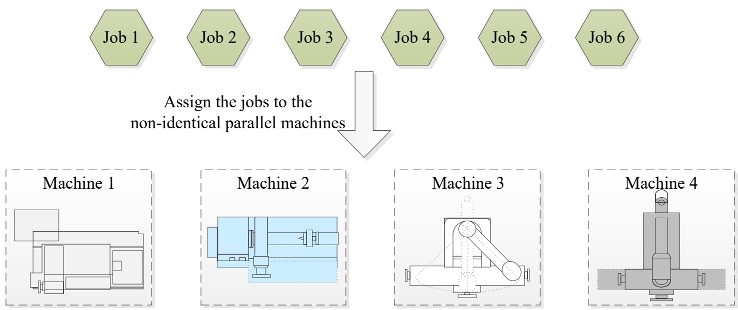

Figure 2. Classic non-identical parallel machine production in workshop.

3.2. Multi-Objective Model Formulation

Based on classic non-identical parallel machine scheduling, we constructed the multi-objective model of the EHQCCSP.

Calculation of operation time and energy consumption

(1) For the qth HQC, the moving time between two bays on the rail is calculated as follows:

$$\sigma_{b'bq} = D\left|b' - b\right| / V_1^q \tag{1}$$

where $\sigma_{b'bq}$ is the qth HQC's moving time between bays b and b'. When b is the first bay operated by the qth HQC, b' is a dummy bay, and $b' = 0$.

The moving energy consumption of the HQCs on the rail between two bays is calculated below:

$$E_{b'bq} = \sigma_{b'bq} P_1^q \tag{2}$$

(2) The no-load operating time and energy consumption for unloading a container

The no-load operation for unloading a container includes three processes, i.e., a no-load lifting process, a no-load moving process, and a no-load lowering process. For an HQC, the times for the three no-load processes are defined as follows:

$$\zeta_{bcq}^{H1} = \begin{cases} 0, \text{ if the container } c \text{ is the first on} \\ \text{e to be operated by the } q\text{th HQC} \\ \frac{L-l_3}{V_{31}^q}, \text{ otherwise} \end{cases} \tag{3}$$

$$\zeta_{bcq}^{T} = \left(\frac{a_1}{2} + a_2 + \Delta + x_c^b l_2\right) / V_{21}^q \tag{4}$$

$$\zeta_{bcq}^{H2} = \frac{Q_b + (z_c^b - 1) l_3}{V_{31}^q} + t_0 \tag{5}$$

$$\eta_{bcq} = \zeta_{bcq}^{H1} + \zeta_{bcq}^{T} + \zeta_{bcq}^{H2} \tag{6}$$

where ζ_{bcq}^{H1} and ζ_{bcq}^{H2} are the no-load lifting and lowering times of the qth HQC's HM, respectively. ζ_{bcq}^{T} is the no-load moving time of the qth HQC's trolley. η_{bcq} is the total no-load time of the qth HQC for unloading container c.

The energy consumption of the three no-load processes is defined as follows:

$$E_{bcq}^{n} = \zeta_{bcq}^{H1} P_{31}^q + \zeta_{bcq}^{T} P_{21}^q + \zeta_{bcq}^{H2} P_{31}^q \tag{7}$$

(3) The heavy-load operating time and energy consumption for unloading a container

Three processes are included in the heavy-load operation, i.e., the heavy-load lifting process, the heavy-load moving process, and the heavy-load lowering process. The times of the three heavy-load processes for an HQC operating a container are given as follows:

$$\xi_{bcq}^{H1} = (Q_b - (N_b - 1) l_3 + z_c^b l_3) / V_{32}^q \tag{8}$$

$$\xi_{bcq}^{T} = \left(\frac{a_1}{2} + a_2 + \Delta + x_c^b l_2\right) / V_{22}^q \tag{9}$$

$$\xi_{bcq}^{H2} = (L - l_3) / V_{32}^q + t_0 \tag{10}$$

$$\chi_{bcq} = \xi_{bcq}^{H1} + \xi_{bcq}^{T} + \xi_{bcq}^{H2} \tag{11}$$

where ξ_{bcq}^{H1} and ξ_{bcq}^{H2} are the heavy-load lifting and lowering times of the qth HQC's HM, respectively. ξ_{bcq}^{T} is the heavy-load moving time of the qth HQC's trolley. χ_{bcq} is the total heavy-load operating time of the qth HQC for unloading container c.

The heavy-load energy consumption of the qth HQC for operating a container is calculated below:

$$E_{bcq}^{l} = \xi_{bcq}^{H1} P_{32}^q + \xi_{bcq}^{T} P_{22}^q + \xi_{bcq}^{H2} P_{32}^q \tag{12}$$

Objective functions

The three objective functions considered in this paper are defined as follows:

$$min\{C_{max}, ATQ, ECQ\} \tag{13}$$

$$C_{max} = max\{C_c | c = 1, 2, \ldots, n\} \quad (14)$$

$$ATQ = \frac{1}{m} \sum_{q=1}^{m} Q_q^T \quad (15)$$

$$ECQ = E_1 + E_2 + E_3 \quad (16)$$

$$E_1 = \sum_{q=1}^{m} \sum_{b',b \in \theta_q} y_{b'bq} E_{b'bq} \quad (17)$$

$$E_2 = \sum_{c=1}^{n} \sum_{q=1}^{m} x_{cq} E_{bcq}^{n} \quad (18)$$

$$E_3 = \sum_{c=1}^{n} \sum_{q=1}^{m} x_{cq} E_{bcq}^{l} \quad (19)$$

Equation (13) represents three objective functions that need to be minimized simultaneously. Equation (14) is the maximum completion time (C_{max}) of all containers, which means the completion time of the HQC for the last container. This is the most frequently used objective in QC scheduling and usually evaluates the unloading efficiency. Equation (15) calculates the average operation time of HQCs (ATQ), which is important for balancing the workload of HQCs. Equation (16) represents the total energy consumption of all container tasks by HQCs (ECQ), which is another major concern for port operators due to environmental pollution and limited energy resources. The ECQ consists of three components: the total moving energy consumption of all HQCs on the rail (E_1), calculated after completing traveling operations using Equation (17); the total energy consumption of all HQCs (E_2), calculated after the no-load handling operations within containers using Equation (18); and the total energy consumption of HQCs (E_3), calculated after the heavy-load operation with containers using Equation (19).

Constraints

$$C_{max} \geq C_c; \forall c \in \{1, 2, \ldots, n\} \quad (20)$$

$$\begin{gathered} C_{c'} + \eta_{bcq} + \chi_{bcq} \leq C_c + \left(1 - z_{c'cq}\right) H \\ \forall c \neq c'; \forall c, c' \in \{1, 2, \ldots, n\}; \forall b \in \{1, 2, \ldots, B\}; \\ \forall q \in \{1, 2, \ldots, m\} \end{gathered} \quad (21)$$

$$\begin{gathered} G_{b'} + \sum_{c=1}^{\omega_b} \left(\eta_{bcq} + \chi_{bcq}\right) + \sigma_{b'bq} \leq G_b + \left(1 - y_{b'bq}\right) H \\ \forall b \neq b'; \forall b, b' \in \{1, 2, \ldots, B\}; \forall q \in \{1, 2, \ldots, m\} \end{gathered} \quad (22)$$

$$\begin{gathered} H(\mu_{bk} + \mu_{kb}) \geq \sum_{b=1}^{B} b\, d_{bq} - \sum_{k=1}^{B} k\, d_{kq'} + h \\ \forall b < k; \forall q < q'; \forall q, q' \in \{1, 2, \ldots, m\} \end{gathered} \quad (23)$$

$$\sum_{c=1}^{n} x_{cq} = 1; \forall q \in \{1, 2, \ldots, m\} \quad (24)$$

$$\sum_{q=1}^{m} x_{cq} = 1; \forall c \in \{1, 2, \ldots, n\} \quad (25)$$

$$\sum_{b'=1}^{B} y_{b'bq} = 1; \forall b \in \{1, 2, \ldots, B\}; \forall q \in \{1, 2, \ldots, m\} \quad (26)$$

$$\sum_{b=1}^{B} y_{b'bq} = 1; \forall b' \in \{1, 2, \ldots, B\}; \forall q \in \{1, 2, \ldots, m\} \quad (27)$$

$$\sum_{c'=0}^{n} z_{c'cq} = 1; \forall c \in \{1, 2, \ldots, n\}; \forall q \in \{1, 2, \ldots, m\} \quad (28)$$

$$\sum_{c=1}^{n} z_{c'cq} = 1; \forall c' \in \{0,1,2,\ldots,n\}; \forall q \in \{1,2,\ldots,m\} \tag{29}$$

$$\sum_{b=1}^{B} d_{bq} = 1; \forall q \in \{1,2,\ldots,m\} \tag{30}$$

$$\sum_{q=1}^{m} d_{bq} = 1; \forall b \in \{1,2,\ldots,B\} \tag{31}$$

$$\begin{gathered} x_{cq}, d_{bq}, \mu_{bk}, y_{b'bq}, z_{c'cq} \in \{0,1\} \\ \forall c, c' \in \{1,2,\ldots,n\}; \forall b, k, b' \in \{1,2,\ldots,B\}; \forall q \in \{1,2,\ldots,m\} \end{gathered} \tag{32}$$

Constraint (20) ensures that the completion time of a container is not greater than C_{max}. Constraint (21) ensures that one container can be operated only after its predecessor is unloaded. Constraint (22) indicates that, when two bay tasks are assigned to an HQC, the second bay task can be unloaded only after its predecessor is completed and the movement of the HQC on the rail is completed. Constraint (23) is the cooperative operational constraint that guarantees the safety margin distance of HQCs. When two bay tasks b and k ($b < k$) are operated by two HQCs q and q', respectively, with an overlapping period, $\mu_{bk} + \mu_{kb} = 0$. Since the bays and the HQCs are numbered in the same direction, $k - b \geq h$ is satisfied. This ensures that the two HQCs q and q' with an overlapping operation period must maintain a safety margin of at least h bays. Constraint (24) indicates that one HQC can only unload one container at a time, and constraint (25) ensures that one container can only be allocated to one HQC. Constraint (26) ensures that a bay task must follow one and only one predecessor, except when it is the first bay task to be unloaded on the HQC. Constraint (27) means that if a bay task has been unloaded on an HQC, one and only one different bay task can be selected for unloading next, except when it is the last bay task to be unloaded on the HQC. Constraint (28) specifies that a container must follow one and only one predecessor, except when it is the first container to be unloaded on the HQC. Constraint (29) means that if a container has been unloaded on an HQC, one and only one different container can be selected for unloading next, except when it is the last container to be unloaded on the HQC. Constraint (30) implies that one HQC can only unload one bay task at a time, and constraint (31) ensures that one bay task can only be unloaded by one HQC at a time. Constraint (32) specifies the ranges of decision variables.

4. Proposed EMOEA

In this section, we describe the proposed EMOEA for the EHQCCSP. Based on the EHQCCSP features, we designed effective encoding and population initialization as well as decoding methods. A cooperative operation strategy was adopted to maintain the safety margin. We designed specific evolution operators in the EMOEA so that it is suitable for the EHQCCSP. In addition, an opposition-based learning (OBL) strategy was adopted to improve the EMOEA's local search ability.

4.1. Population Initialization and Encoding

As mentioned in Section 3.2, the EHQCCSP needs to solve two sub-problems, i.e., (1) divide the bays and allocate them to the given HQCs and (2) arrange the bays for each HQC. The two sub-problems are interrelated. The second sub-problem depends on the first sub-problem. The encoding of the two sub-problems forms a complete solution. In this paper, we use $\boldsymbol{X} = [\boldsymbol{A}, \boldsymbol{B}]$ to represent a complete solution of the EHQCCSP. $\boldsymbol{A}$ is the encoding for the first sub-problem, and $\boldsymbol{B}$ is the encoding for the second sub-problem. We propose an effective method to achieve the representation of a complete solution. As mentioned before, the container sequence in a bay has no impact on the operation time and energy consumption. Therefore, we do not need specific techniques to encode the container sequence. In this work, the containers in each bay are arranged in a random manner.

For the first sub-problem, the encoding process is described as follows:

Step 1: m increasing integers, i.e., $I_1, I_2, \ldots, I_m$, in the interval [1, B] are randomly obtained. m is the number of HQCs, and B is the number of bays. Then, an encoding for bay segmentation (denoted as $\boldsymbol{A}$) is obtained by the m increasing integers. With this encoding, the set of bays that will be operated by each HQC can be identified. For instance, the set of bays that will be operated by the first HQC is $[1, 2, \ldots, I_1]$, and the set of bays that will be operated by the second HQC is $[I_1 + 1, \ldots, I_2]$. By analogy, the bay set for the mth HQC is $[I_{m-1} + 1, \ldots, I_m]$.

Step 2: The bays to be operated by each HQC are then randomly arranged. All of the bays are arranged and combined from left to right. Then, an encoding for the bay arrangement (denoted as $\boldsymbol{B}$) is obtained.

Step 3: $\boldsymbol{A}$ and $\boldsymbol{B}$ are combined to generate a complete solution, i.e., $\boldsymbol{X} = [\boldsymbol{A}, \boldsymbol{B}]$.

In order to maintain the safety margin, the encoded $\boldsymbol{X}$ needs to be checked and adjusted by using a cooperative operation strategy, which is described in Section 4.2. By repeating the above process N times, an initial population with N feasible solutions can be obtained.

To have a better understanding of the above encoding method, a small-sized instance with three HQCs and six bays is used as an example and is presented in Figure S2 in the Supplementary File. The feasible solution shown in Figure S2 is revealed from Figure S1.

4.2. Cooperative Operation Strategy

In the current population, there may be some infeasible solutions because of the constraint of the safety margin distance. Hence, we have to check the solutions so that the infeasible solutions become feasible ones. To this end, we propose a cooperative operation strategy. The detailed procedure of this strategy for a complete solution $\boldsymbol{X} = [\boldsymbol{A}, \boldsymbol{B}]$ is as follows:

Step 1: In bay arrangement $\boldsymbol{B}$, the first bay (denoted as b_q^1) operated by HQC q and the first bay (denoted as b_{q+1}^1) operated by HQC $q + 1$ ($1 \leq q \leq m - 1$), respectively, are determined.

Step 2: If $\left| b_q^1 - b_{q+1}^1 \right| \leq h$, the constraint of safety margin distance is not satisfied. It is necessary to adjust the bays in $\boldsymbol{B}$. Figure S3 in the Supplementary File presents an example of bay division and arrangement. There are six kinds of bay arrangements in this example.

Step 3: For solution $\boldsymbol{X}$, the starting and ending times of all bays operated by each HQC are calculated with the model proposed in Section 3.2. Via Equation (23), judge whether two adjacent HQCs q and q' with an overlapping operation time period maintain a safety margin distance of at least h bays. If Equation (23) is not satisfied, a new solution is generated via the method in Section 4.1 until it is feasible.

4.3. Decoding

The aim of decoding is to determine the starting and ending operation times of HQCs for containers and bays in one encoded solution. In the meanwhile, three objective function values (i.e., C_{max}, ATQ, and ECQ) need to be computed. An active decoding method is used in this paper. The detailed decoding steps are as follows:

Step 1: The bay set and arrangement for each HQC are determined. For HQC q, its operation bay permutation is scanned from left to right. For a scanned bay b, its container sequence is scanned from left to right.

Step 2: The completion time (denoted by $C_{c'}$) is determined for operating container c' with HQC q. Container c' is operated before container c with HQC q. If container c' is the last container to be operated in a bay, the completion time of the bay is $C_{c'}$.

Step 3: The starting and ending times are determined for operating container c with HQC q. If container c' is the last container to be operated in a bay, the no-load starting time for operating the first container c in the bth bay is $S_c^n = C_{c'} + D * \left| b' - b \right| / V_1^q$, and the no-load ending time for operating container c in the bth bay is $E_c^n = S_c^n + \eta_{bcq}$; the heavy-load starting time for operating the first container c in the bth bay is $S_c^l = E_c^n$, and the heavy-load ending time for operating container c in the bth bay is $E_c^l = S_c^l + \chi_{bcq}$. If container c' is not the last container to be operated in a bay, the no-load starting time for operating container c in the bay is $S_c^n = C_{c'}$, and the no-load ending time for operating container c in the bay is $E_c^n = S_c^n + \eta_{bcq}$; the heavy-load starting time for operating the first container c in the bay is $S_c^l = E_c^n$, and the heavy-load ending time for operating container c in the bay is $E_c^l = S_c^l + \chi_{bcq}$.

Step 4: The starting and ending times are determined for all HQCs during the moving process on the rail and the no-load and heavy-load processes for operating containers. Thereafter, the three objective function values, i.e., C_{max}, ATQ, and ECQ, are calculated according to Equations (14)–(19). Finally, the solution of the studied problem is decoded.

4.4. Fuzzy-Correlation-Entropy-Based Fitness Evaluation Mechanism

FEM is the key factor that affects a multi-objective optimization algorithm's performance. A good FEM can enhance the convergence of an algorithm.

To overcome the drawbacks of scalar-based FEM and non-dominated-sorting-based FEM, we adopted fuzzy correlation entropy (FCE) to enhance FEMs [33]. Currently, no studies in the literature use FCE-based FEM to solve the QCSP with multiple objectives. Motivated by the potential of FCE-based FEM, we attempt to integrate this novel FEM into the evolutionary algorithm so as to evaluate and select solutions to our EHQCCSP. According to the literature [14,33], first, the reference points are constructed using the dynamic construction method; second, the fuzzy sets are constructed in order to establish the connection between MOP and fuzzy set theory; finally, the similarity relationship between individual and reference points is determined using FCE.

4.5. Problem-Feature-Based Evolutionary Operators

4.5.1. Crossover

Due to the uniqueness of the EHQCCSP, it is necessary to adopt a specific crossover operation with a certain probability for the problem. It should be noted that these existing crossover operations cannot be applied to our EHQCCSP directly. As mentioned before, the EHQCCSP involves two sub-problems with different structures, i.e., bay division and arrangement. Note that no crossover operation is conducted on the container sequence because it has no impact on operational efficiency and energy consumption. In this study, we propose an effective crossover operation for bay division and arrangement. The detailed crossover process is presented as follows:

Step 1: Two parent individuals are randomly selected from the current population. The two parent individuals are referred to as $\boldsymbol{PX}_1$ and $\boldsymbol{PX}_2$. For $\boldsymbol{PX}_1$ and $\boldsymbol{PX}_2$, their bay division parts are referred to as $\boldsymbol{PA}_1$ and $\boldsymbol{PA}_2$, respectively; their bay arrangement parts are referred to as $\boldsymbol{PB}_1$ and $\boldsymbol{PB}_2$, respectively.

Step 2: Two integers, a_1 and a_2, are randomly generated for the bay division part and satisfy $0 < a_1 < a_2 < D_1$. D_1 is the length of the bay division part. Likewise, two integers, b_1 and b_2, are randomly generated for the bay arrangement part and satisfy $0 < b_1 < b_2 < D_2$, where D_2 is the length of the bay arrangement part. After that, the genes between a_1 and a_2 in $\boldsymbol{PA}_1$ and $\boldsymbol{PA}_2$ are exchanged; the genes between b_1 and b_2 in $\boldsymbol{PB}_1$ and $\boldsymbol{PB}_2$ are also exchanged.

Step 3: After crossover, two intermediate individuals (i.e., $\boldsymbol{IX}_1$ and $\boldsymbol{IX}_2$) for the bay division and arrangement are obtained. Note that $\boldsymbol{IX}_1$ and $\boldsymbol{IX}_2$ may be infeasible for the EHQCCSP. It is necessary to adjust and repair $\boldsymbol{IX}_1$ and $\boldsymbol{IX}_2$. We first identify the duplicate genes in $\boldsymbol{IX}_1$ and $\boldsymbol{IX}_2$ and then replace them with the genes missed in $\boldsymbol{IX}_1$ and $\boldsymbol{IX}_2$. In addition, we need to ensure that $\boldsymbol{IX}_1$ and $\boldsymbol{IX}_2$ satisfy the constraint of the safety margin via the cooperative strategy in Section 4.2. At last, we will obtain two offspring individuals, referred to as $\boldsymbol{OX}_1$ and $\boldsymbol{OX}_2$.

With the crossover operation for bay division and arrangement, an example is presented, as shown in Figure S6.

4.5.2. Mutation

After crossover, the mutation operation is carried out with a certain probability to obtain a more diversified population of individuals. The mutation process for an individual is as follows:

Step 1: For a selected parent individual, referred to as $\boldsymbol{PX}$, its bay division part is referred to as $\boldsymbol{PA}$, and its bay arrangement part is referred to as $\boldsymbol{PB}$.

Step 2: Position k in $\boldsymbol{PA}$ and gene I_k corresponding to position k are selected. Gene I_{k-1} at position $k-1$ and gene I_{k+1} at position $k+1$ are determined. A random disturbance is applied to gene I_k to obtain a new gene in the interval $[I_{k-1}, I_{k+1}]$.

Step 3: The bay arrangement is re-arranged and adjusted according to the new bay division $\boldsymbol{PA}$, and an intermediate individual $\boldsymbol{IX}$ is obtained.

Step 4: Whether $\boldsymbol{IX}$ maintains the safety margin distance is determined. If the safety margin distance is not satisfied, $\boldsymbol{IX}$ is adjusted to obtain a feasible $\boldsymbol{OX}$.

It should be noted that, like the crossover, the mutation operator is not executed on the container operation sequence. Figure S5 presents an example of the mutation operation for a feasible individual.

4.5.3. Opposition-Based Learning

In this paper, we employ the OBL strategy to improve the diversity of population solutions and enhance the exploitation ability of the EMOEA.

There are no studies on adopting the OBL strategy in a MOEA to solve the EHQCCSP. Note that the EHQCCSP has two sub-problems with different constraints and upper and lower bounds. This means that the basic OBL needs to be changed according to the nature of the EHQCCSP. For a solution $\boldsymbol{X} = [\boldsymbol{A}, \boldsymbol{B}]$ in the current population, the OBL procedure is presented as follows:

Step 1: The upper and lower bounds, referred to as U_{1s} and L_{1s}, are determined for the sth dimension of the bay division part $\boldsymbol{A}$. In the EHQCCSP, each dimension of the bay division $\boldsymbol{A}$ varies in the interval $[1, B]$. Hence, we have $U_{1s} = B$ and $L_{1s} = 1$. The upper and lower bounds, referred to as U_{2s} and L_{2s}, are determined for the sth dimension of the bay arrangement part $\boldsymbol{B}$. Likewise, we have $U_{2s} = B$ and $L_{2s} = 1$.

Step 2: OBL is conducted on the bay division part $\boldsymbol{A}$ and the arrangement part $\boldsymbol{B}$. Then, the opposite bay division part $\boldsymbol{A}'$ and the opposite bay arrangement part $\boldsymbol{B}'$ are obtained.

Step 3: $\boldsymbol{A}'$ is sorted in ascending order. As per the sorted $\boldsymbol{A}'$, the bay arrangement for each QC is scanned from left to right. And then, a new bay arrangement for each QC is obtained. At last, a feasible opposite solution $\boldsymbol{X}'$ is generated.

Figure S6 shows an example of OBL for a solution. Again, the OBL strategy is not conducted on the container operation sequence.

When the OBL strategy is adopted in the EMOEA, the quality of the solutions and the convergence of the EMOEA can be improved. However, when OBL is incorporated into the EMOEA, it will increase the computation time, especially for large-scale problems. With this in mind, we only conduct OBL on the best $r \times 100\%$ solutions in the current population. The best $r \times 100\%$ solutions are selected by the FCE-based FEM.

5. Experiments and Result Analysis

In order to evaluate the effectiveness and efficiency of the proposed EMOEA in solving the EHQCCSP, a series of experiments were designed and are described in this section. For fair comparisons, all relevant algorithms were limited to $OH(n)$ seconds for each instance, where n is the number of containers. And each instance was independently run 30 times. All the algorithms were coded in MATLAB R2014a and executed on a computer with an Intel Core i7 CPU of 4.00 GHz and 16.0 GB RAM.

5.1. Test Instances

Note that there are no studies that use the same problem as our EHQCCSP. The required instances were generated based on the physical model of the Dalian container terminal in China. According to the real-world data collected for the Dalian container terminal, ten numerical instances with different scales were generated. We used the combination symbol "$n \times m \times B$" to represent each instance, where n is the number of containers, m is the number of QCs, and B is the number of bays in the vessel. The sizes of the ten generated instances include $72 \times 3 \times 6$, $120 \times 3 \times 6$, $300 \times 3 \times 6$, $480 \times 4 \times 12$, $720 \times 4 \times 12$, $960 \times 4 \times 12$, $480 \times 6 \times 12$, $960 \times 6 \times 12$, $1200 \times 6 \times 24$, and $2400 \times 6 \times 24$. All of the containers are standard 40ft. The parameter configuration for the EHQCCSP is given in Table S1 in the Supplementary File.

5.2. Performance Metrics

In general, a solution set should be assessed from several aspects, for example, convergence, diversity, and distribution uniformity. In particular, convergence is the most important one for real-world engineering optimization problems. To this end, the hypervolume (HV), inverted generation distance (IGD), and C-metric were adopted in this study as performance metrics to evaluate the performance of the relevant algorithms. The introduced tree metrics are shown in Section S3 in the Supplementary File.

5.3. Comparison with Other Algorithms

To test the effectiveness of the proposed EMOEA in solving the EHQCCSP, the proposed EMOEA was compared with the baseline multi-objective algorithms MOEA/D [34], NSGA-II [35], and SPEA-II [36].

We utilized a Taguchi analysis method [20] to obtain the best parameter combination for the proposed EMOEA and each compared algorithm. A detailed description is presented in Section S4 of the Supplementary File. After the Taguchi analysis, the parameter combination of the EMOEA was set as follows: $N = 40$, $Pc = 0.7$, $Pm = 0.2$, $\alpha = 0.4$, $\beta = 1.1$, and $r = 0.4$. The parameter values of MOEA/D, NSGA-II, and SPEA-II are as follows: $N = 60$, $Pc = 0.8$, $Pm = 0.3$, $\eta_c = 20$, and $\eta_m = 10$ for NSGA-II; $N = 91$, $Pc = 0.9$, $Pm = 0.2$, $\eta_c = 20$, $\eta_m = 20$, and $T = 20$ for MOEA/D; and $N = 80$, $Pc = 0.9$, $Pm = 0.1$, $\eta_c = 20$, set $\eta_m = 10$ for SPEA-II. Here, N is the population size, Pc is the crossover probability, Pm is the mutation probability, α and β are the lower- and upper-bound factors in FCE-based FEM, r is the proportion of solutions implementing the OBL strategy, η_c is the distribution index in the simulated binary crossover, η_m is the distribution index in polynomial mutation, and T is the neighborhood size. In addition, we used the Tchebycheff approach [30] as the scalarizing function for MOEA/D.

The mean HV and IGD results of EMOEA, MOEA/D, NSGA-II, and SPEA-II are shown in Table 2, where the best result is marked in bold. We can observe that the HV values obtained by the EMOEA were larger than those obtained by the other algorithms for all 10 instances. Moreover, the IGD results shown in Table 2 indicate that the EMOEA performed the best in eight instances. The EMOEA performed significantly better than the other three algorithms, with more than an 80% probability.

Thus, the results in Table 2 imply that the EMOEA was superior to the three compared multi-objective algorithms for the EHQCCSP. The EMOEA performs better in terms of convergence, diversity, and distribution. It should be noted in particular that the EMOEA can achieve the best convergence results (i.e., HV results) in all instances, which is very important for the EHQCCSP.

In Table 3, the C-metric comparison results are listed. The results show that the EMOEA was superior to MOEA/D, NSGA-II, and SPEA-II in all 10 instances. Notably, the C-metric values of the EMOEA were equal to 1 for several instances against SPEA-II, which means that there was at least one solution in the solution set obtained by MOEA that dominated all solutions produced by SPEA-II. Also, from the Wilcoxon rank sum test results, we can find that the EMOEA is better than the other three algorithms for the C-metric in all 10 instances. Therefore, the results in Table 3 indicate that the EMOEA outperforms the three compared algorithms in terms of convergence, which is consistent with the conclusion drawn from the results in Table 3.

Table 2. Performance comparison of the four MOEAs on HV and IGD.

No.	$n \times m \times B$	HV				IGD			
		EMOEA	NSGA-II	MOEA/D	SPEA-II	EMOEA	NSGA-II	MOEA/D	SPEA-II
1	72 × 3 × 6	**1.4723**	1.3060 (+)	1.4130 (+)	0.4113 (+)	**0.0433**	0.0528 (+)	0.0566 (+)	0.0476 (+)
2	120 × 3 × 6	**1.2858**	0.9823 (+)	0.9620 (+)	0.2463 (+)	0.0352	0.0617 (+)	0.0372 (+)	**0.0292 (−)**
3	300 × 3 × 6	**1.4750**	1.0787 (+)	1.4126 (+)	0.3358 (+)	**0.0320**	0.0605 (+)	0.0375 (+)	0.0342 (+)
4	480 × 4 × 12	**1.3520**	1.3075 (+)	1.1668 (+)	0.4965 (+)	**0.0318**	0.0566 (+)	0.0345 (+)	0.0409 (+)
5	720 × 4 × 12	**1.3652**	1.3078 (+)	1.1030 (+)	0.4214 (+)	**0.0413**	0.0632 (+)	0.0472 (+)	0.0396 (−)
6	960 × 4 × 12	**1.3745**	1.2736 (+)	1.0680 (+)	1.0148 (+)	**0.0414**	0.0579 (+)	0.0570 (+)	0.0448 (+)
7	1200 × 6 × 12	**1.4458**	1.2727 (+)	0.9824 (+)	1.0679 (+)	**0.0432**	0.0572 (+)	0.0523 (+)	0.0541 (+)
8	2400 × 6 × 12	**1.2360**	0.7960 (+)	1.0090 (+)	1.0611 (+)	**0.0541**	0.0555 (+)	0.0654 (+)	0.0663 (+)
9	1200 × 6 × 24	**1.3437**	1.2544 (+)	1.0754 (+)	1.0394 (+)	**0.0418**	0.0445 (+)	0.0537 (+)	0.0588 (+)
10	2400 × 6 × 24	**1.5952**	1.4195 (+)	1.1772 (+)	0.7355 (+)	**0.0479**	0.0571 (+)	0.0582 (+)	0.0664 (+)

Note: best results are marked in bold for each instance.

Table 3. Performance comparison of the four MOEAs for C-metric.

No.	$n \times m \times B$	*C*-Metric					
		EMOEA (E) vs. NSGA-II (N)		EMOEA (E) vs. MOEA/D (M)		EMOEA (E) vs. SPEA-II (S)	
		C(E,N)	*C*(N,E)	*C*(E,M)	*C*(M,E)	*C*(E,S)	*C*(S,E)
1	72 × 3 × 6	**0.5476**	0.0820 (+)	**0.7600**	0.0204 (+)	**0.8543**	0.0000 (+)
2	120 × 3 × 6	**0.4898**	0.0502 (+)	**0.7885**	0.0100 (+)	**0.8600**	0.0000 (+)
3	300 × 3 × 6	**0.7234**	0.0000 (+)	**0.8784**	0.0000 (+)	**1.0000**	0.0000 (+)
4	480 × 4 × 12	**0.6845**	0.0000 (+)	**0.7576**	0.0000 (+)	**1.0000**	0.0000 (+)
5	720 × 4 × 12	**0.6526**	0.0000 (+)	**0.6878**	0.0000 (+)	**1.0000**	0.0000 (+)
6	960 × 4 × 12	**0.5872**	0.0000 (+)	**0.8733**	0.0000 (+)	**1.0000**	0.0000 (+)
7	1200 × 6 × 12	**0.5515**	0.0000 (+)	**0.8546**	0.0000 (+)	**0.8017**	0.0000 (+)
8	2400 × 6 × 12	**0.6780**	0.0000 (+)	**0.6444**	0.0000 (+)	**0.6078**	0.0000 (+)
9	1200 × 6 × 24	**0.6012**	0.0000 (+)	**0.7136**	0.0000 (+)	**0.7775**	0.0000 (+)
10	2400 × 6 × 24	**0.6464**	0.0000 (+)	**0.7878**	0.0000 (+)	**0.9270**	0.0000 (+)

Note: best results are marked in bold for each instance.

The above results show that the EMOEA performs better than its three peers in terms of convergence, diversity, and distribution. This implies that the EMOEA can provide a better candidate solution set for the studied multi-objective optimization problem—the EHQCCSP.

5.4. How to Select an Appropriate Schedule from the Final Solution Set

It should be noted that the proposed EMOEA and its peers are population-based algorithms. After the optimization of population-based algorithms is completed, a final solution set containing several excellent solutions is output. However, for engineering optimization problems, e.g., the EHQCCSP in this work, the decision makers only need an appropriate scheme (solution). Hence, it is very important to select a good solution from the final solution set by using a simple and effective solution selection method. In our EMOEA, we use the FCE-based FEM to evaluate the evolution population and select an appropriate solution from the final solution set. The solution with the largest fuzzy correlation entropy coefficient (i.e., ρ) is regarded as the best one. We utilized a small instance, i.e., instance 1, to show the selection process of the EMOEA.

Table 4 lists the objective values of the solutions in the final solution set obtained by the EMOEA. As shown in Table 4, there were 20 solutions in the final solution set, and each solution had a ρ value. We can observe that the 10th solution had the largest ρ value (i.e., 0.9817). Compared to other solutions, this solution can achieve three better objective values as a whole, which are marked in bold in Table 4.

Table 4. The objective values of the solutions obtained by the EMOEA on a small-scale instance.

Solutions	C_{max}(s)	ATQ (s)	ECQ (MJ)	ρ	Solutions	C_{max}(s)	ATQ (s)	ECQ (MJ)	ρ
1	5326	3635	12,380	0.7756	11	5246	3581	22,512	0.7263
2	5263	3587	35,989	0.5616	12	3843	3627	32,357	0.7001
3	5263	3634	12,470	0.7913	13	5335	3588	11,814	0.7727
4	5263	3587	23,356	0.7143	14	5254	3584	43,378	0.4577
5	3852	3680	14,848	0.9743	15	3852	3633	20,902	0.8918
6	5326	3586	28,779	0.6427	16	5318	3583	35,898	0.5562
7	5335	3591	11,969	0.7732	17	5335	3588	11,815	0.7727
8	5246	3628	19,114	0.7593	18	5263	3634	12,472	0.7913
9	5254	3631	38,988	0.5218	19	5326	3635	14,857	0.7710
10	**4156**	**3636**	**12,697**	**0.9817**	20	5326	3638	12,621	0.7758

Note: best results are marked in bold for each instance.

Figure 3 depicts the three objective values of the preferable solutions selected from the final solution sets of the four multi-objective algorithms when solving four instances with different scales, i.e., instances 1, 4, 8, and 9. The three compared algorithms used their own fitness evaluation mechanisms to select the best solutions from their final solution sets. It is revealed in Figure 3 that the three objective values of the best solution of the EMOEA were better than those of its three peers. The results in Figure 3 further show the superiority of the solution evaluation and the selection mechanism of the EMOEA.

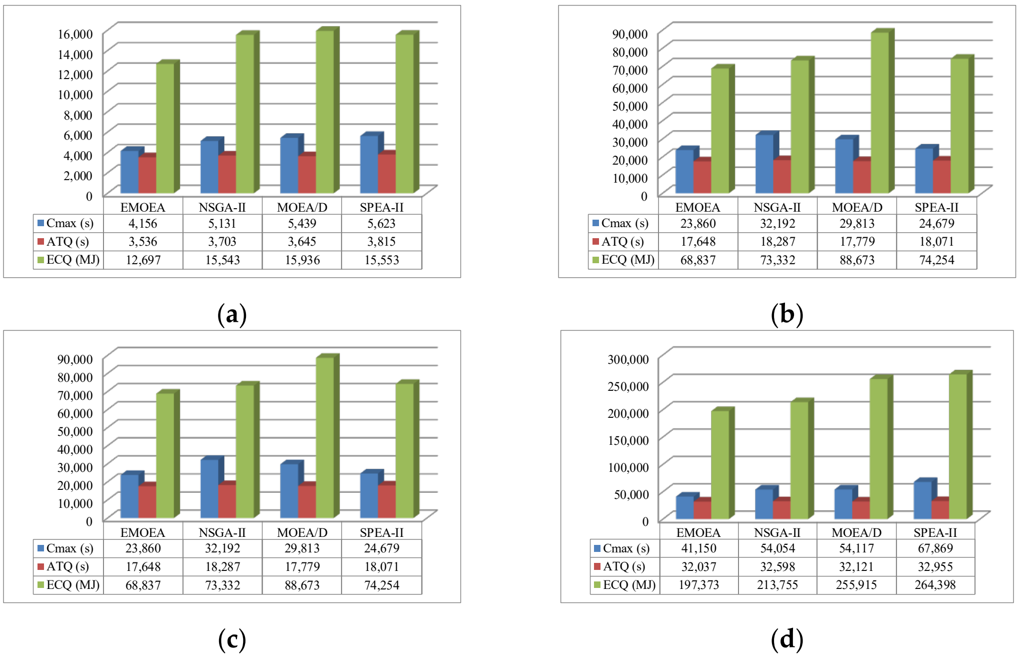

Figure 3. The objective values of the preferable solutions obtained by four MOEAs. (**a**) Instance 1; (**b**) instance 4; (**c**) instance 8; (**d**) instance 9.

Figure 4 is the Gantt chart of the selected best solution, in which the bay division and the container operation sequence are presented. In Figure 4, the red boxes represent the movement operations of HQCs on the rail, the gray boxes denote the no-load processes of HQCs for operating containers, and the white boxes indicate the heavy-load processes of HQCs for operating containers.

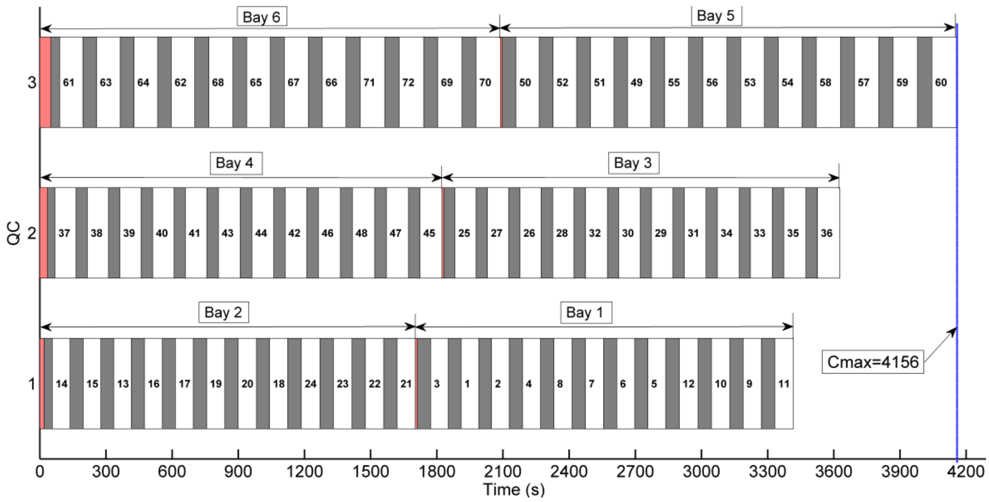

Figure 4. The Gantt chart obtained by EMOEA on instance 1.

Based on the above experiments and analysis, it can be seen that the proposed EMOEA is able to outperform the other three well-known multi-objective algorithms, i.e., NSGA-II, MOEA/D, and SPEA-II, in solving the EHQCCSP. Moreover, the solution evaluation and selection mechanism of the EMOEA can help the decision makers for the EHQCCSP choose an appropriate scheme more conveniently and effectively.

5.5. Practical and Theoretical Implications

The designed EMOEA can solve the EHOCCSP effectively and provide satisfactory solutions to container terminal managers. Based on the final solutions (e.g., the Gantt chart), the processing sequence of containers and the assignments of HQCs can be determined. This can provide excellent schemes to managers to achieve short processing times, low energy consumption, and balanced operations. Therefore, our research is of great significance in improving the competitiveness of container terminals, promoting economic development, and encouraging energy conservation.

6. Conclusions and Further Work

The contributions of this paper to the literature are as follows. From an academic standpoint, we studied an energy-efficient heterogeneous quay crane cooperative scheduling problem (EHQCCSP) considering their movement constraints in the container terminal, where various operational capacities of heterogeneous QCs were considered. A multi-objective mathematical model for the EHQCCSP was built, aiming to simultaneously minimize the maximum completion time of all containers, the average completion time of HQCs, and the total energy consumption of HQCs while maintaining safety. To better solve the EHQCCSP, the EMOEA was proposed. The EMOEA encodes and initializes the population based on a problem-feature-based method. An effective cooperative operation strategy for HQCs was adopted. A novel FCE-based FEM was used to evaluate and sort the population solutions. OBL improved the quality and diversity of the solutions. From a practical perspective, the proposed model incorporates real-life operational issues, such as how to dispatch heterogeneous QCs with three trade-off objectives. The findings will benefit terminal managers in their day-to-day operations.

Comparative experiments verified the accuracy of the EHQCCSP. An analysis was conducted to study the impact of various operational capacities of HQCs on the three studied objectives. The results of the analysis revealed that the different operational capacities of HQCs had a significant impact on the three studied objectives, especially for some large-scale problems. The experimental results also indicate that the EMOEA was able to be superior to three well-known multi-objective algorithms in solving the

EHQCCSP under consideration. This study will be extremely useful to modern green container terminals in which HQCs are used and energy conservation is pursued.

In this paper, each task group's handling volume is deterministic. However, in reality, it may fluctuate and cannot be predicted accurately. And the HQC productivity is affected by various external factors, such as machine failures, the early arrival of vessels, etc. Therefore, it will be important to consider uncertain events for the EHQCCSP in the future. In addition, some more efficient methods should be designed for the large-scale EHQCCSP, considering the significant increase in calculation time when the problem scale increases.

Supplementary Materials: The following supporting information can be downloaded at https://www.mdpi.com/article/10.3390/jmse11101884/s1. Figure S1. The framework of the EMOEA. Figure S2. An example of encoding. Figure S3. An example of feasible and infeasible solutions. Figure S4. An example for crossover. Figure S5. Mutation for bay division and arrangement part. Figure S6. OBL strategy for a solution. Figure S7. The trends of factor levels for key parameters. Table S1. Parameter configuration of numerical experiments

Author Contributions: Conceptualization, L.Z., L.H. and Y.Z. (Yu Zhang); funding acquisition, Y.Z. (Yu Zhang), Y.Z. (Yong Zhou) and W.L.; investigation, L.Z., L.H. and Y.L.; methodology, L.Z., L.H. and Y.Z. (Yu Zhang); project administration, Y.Z. (Yu Zhang), Y.Z. (Yong Zhou) and W.L.; software, L.H. and Y.L.; supervision, Y.Z. (Yu Zhang) and W.L.; writing—original draft, L.Z. and L.H.; writing—review and editing, L.Z. and L.H. All authors have read and agreed to the published version of the manuscript.

Funding: This work was supported by the National Natural Science Foundation of China (Grants 62173263 and 72174160), the National Key Research and Development Program of China (2019YFB1600400), and the Innovation Research Team Project of Natural Science Foundation of Hainan, China (621CXTD1013).

Institutional Review Board Statement: Not applicable.

Informed Consent Statement: Not applicable.

Data Availability Statement: The data presented in this study are available on request from the corresponding author. The data are not publicly available due to limitations of the study phase.

Conflicts of Interest: The authors declare no conflict of interest.

Abbreviations

Notations

q, q':	The index of HQCs
b, b', k:	The index of bays
c, c':	The index of containers
n:	The number of containers
m:	The number of HQCs
B:	The number of bays
θ_q:	The set containing the bays processed by the qth HQC
$S^1_{b'bq}$:	The start time of the qth HQC moving from the b'th bay to the bth bay; if the bth bay is the first one to be operated on the qth HQC, bay $b' = 0$, which means that b' is a dummy bay
S^n_{bcq}:	The start time of the qth HQC moving to a position of container c in the bth bay with no load
S^l_{bcq}:	The start time of the qth HQC for processing container c in the bth bay with a heavy load
h:	The minimum number of bays to maintain the safety margin distance between two adjacent HQCs
ω_b:	The number of containers at the bth bay
Δ:	The clearance between the vessel and landside
V^q_1:	The moving speed of the qth HQC on the rail
V^q_{21}:	The moving speed of the qth HQC's trolley with no load
V^q_{22}:	The moving speed of the qth HQC's trolley with a heavy load
V^q_{31}:	The lifting and lowering speed of the qth HQC's HM with no load

V_{32}^{q}:	The lifting and lowering speed of the qth HQC's HM with a heavy load
P_{1}^{q}:	The power of the qth HQC when it moves on the rail
P_{21}^{q}:	The moving power of the qth HQC's trolley with no load
P_{22}^{q}:	The moving power of the qth HQC's trolley with a heavy load
P_{31}^{q}:	The lifting and lowering power of the qth HQC's HM with no load
P_{32}^{q}:	The lifting and lowering power of the qth HQC's HM with a heavy load
x_{c}^{b}:	The position of container c in the X-axis direction in the bth bay
z_{c}^{b}:	The position of container c in the Z-axis direction in the bth bay
t_0:	The time required to grab and unlock a container
D:	The length of a bay
L:	The maximum height of an HQC's spreader to the ground
Q_b:	The maximum height of an HQC's spreader to the top of the container in the bth bay
a_1:	The length of the HQC girder
a_2:	The width of the HQC frame
l_1:	The length of a container
l_2:	The width of a container
l_3:	The height of a container
H:	A sufficiently large integer
Decision Variables	
C_{max}:	The maximum completion time of all containers
S_c:	The start time for unloading the cth container
C_c:	The end time for unloading the cth container
G_b:	The completion time of the bth bay
Q_q^T:	The end time of the qth HQC
x_{cq}:	If the cth container is assigned to the qth HQC for unloading, $x_{cq} = 1$; otherwise, $x_{cq} = 0$
d_{bq}:	$d_{bq} = 1$, if the bth bay is assigned to the qth HQC for unloading; $d_{bq} = 0$ otherwise
μ_{bk}:	$\mu_{bk} = 1$ if the start time for unloading the bth bay is not earlier than the end time for unloading the kth bay; $\mu_{bk} = 0$ otherwise
$y_{b'bq}$:	$y_{b'bq} = 1$ if the b'th bay is unloaded before the bth bay on the qth HQC; $y_{b'bq} = 0$ otherwise
$z_{c'cq}$:	$z_{c'cq} = 1$ if the c'th container is unloaded before the cth container on the qth HQC; $z_{c'cq} = 0$ otherwise

References

1. Yang, X.; Mi, W.; Li, X.; An, G.; Zhao, N.; Mi, C. A simulation study on the design of a novel automated container terminal. *IEEE Trans. Intell. Transp. Syst.* **2015**, *16*, 2889–2899. [CrossRef]
2. Tian, C.M.; Yan, W.; Yue, J. Quay crane scheduling in automated container terminal for the trade-off between operation efficiency and energy consumption. *Adv. Eng. Inform.* **2021**, *48*, 101285. [CrossRef]
3. Li, Y.; Chu, F.; Zheng, F.; Liu, M. A Bi-Objective Optimization for Integrated Berth Allocation and Quay Crane Assignment With Preventive Maintenance Activities. *IEEE Trans. Intell. Transp. Syst.* **2022**, *23*, 2938–2955. [CrossRef]
4. Wang, H.; Li, R.; Gong, W. Minimizing tardiness and makespan for distributed heterogeneous unrelated parallel machine scheduling by knowledge and Pareto-based memetic algorithm. *Egypt. Inform. J.* **2023**, *24*, 100383. [CrossRef]
5. Duan, Y.T.; Ren, H.X.; Xu, F.Q.; Yang, X.; Meng, Y. Bi-Objective Integrated Scheduling of Quay Cranes and Automated Guided Vehicles. *J. Mar. Sci. Eng.* **2023**, *11*, 1492. [CrossRef]
6. Aslam, S.; Michaelides, M.P.; Herodotou, H. Berth Allocation Considering Multiple Quays: A Practical Approach Using Cuckoo Search Optimization. *J. Mar. Sci. Eng.* **2023**, *11*, 1280. [CrossRef]
7. Tengecha, N.A.; Zhang, X. An Efficient Algorithm for the Berth and Quay Crane Assignments Considering Operator Performance in Container Terminal Using Particle Swarm Model. *J. Mar. Sci. Eng.* **2022**, *10*, 1232. [CrossRef]
8. Mansouri, S.A.; Lee, H.; Aluko, O. Multi-objective decision supports to enhance environmental sustainability in maritime shipping: A review and future directions. *Transport. Res. Part E* **2015**, *78*, 3–18. [CrossRef]
9. Geerlings, H.; van Duin, R. A new method for assessing CO_2-emissions from container terminals: A promising approach applied in Rotterdam. *J. Clean. Prod.* **2011**, *19*, 657–666. [CrossRef]
10. Hop, D.C.; Van Hop, N.; Anh, T.T.M. Adaptive particle swarm optimization for integrated quay crane and yard truck scheduling problem. *Comput. Ind. Eng.* **2021**, *153*, 107075. [CrossRef]

11. Niu, Y.; Yu, F.; Yao, H.; Yang, Y. Multi-equipment coordinated scheduling strategy of U-shaped automated container terminal considering energy consumption. *Comput. Ind. Eng.* **2022**, *74*, 108804. [CrossRef]
12. Zhang, A.; Zhang, W.; Chen, Y.; Chen, G.; Chen, X. Approximate the scheduling of quay cranes with non-crossing constraints. *Eur. J. Oper. Res.* **2017**, *258*, 820–828. [CrossRef]
13. Rodrigues, F.; Agra, A. An exact robust approach for the integrated berth allocation and quay crane scheduling problem under uncertain arrival times. *Eur. J. Oper. Res.* **2021**, *295*, 499–516. [CrossRef]
14. He, L.J.; Chiong, R.; Li, W.F.; Dhakal, S.; Cao, Y.L.; Zhang, Y. Multiobjective optimization of energy-efficient job-shop scheduling with dynamic reference point-based fuzzy relative entropy. *IEEE Trans. Ind. Inform.* **2021**, *18*, 600–610. [CrossRef]
15. Zhu, G.; He, L.; Ju, X.; Zhang, W. A fitness assignment strategy based on the grey and entropy parallel analysis and its application to MOEA. *Eur. J. Oper. Res.* **2018**, *265*, 813–828. [CrossRef]
16. Wang, L.; Wang, J.J.; Jiang, E. Decomposition based multiobjective evolutionary algorithm with adaptive resource allocation for energy-aware welding shop scheduling problem. *Comput. Ind. Eng.* **2021**, *162*, 107778. [CrossRef]
17. Li, W.F.; He, L.J.; Cao, Y.L. Many-objective evolutionary algorithm with reference point-based fuzzy correlation entropy for energy-efficient job shop scheduling with limited workers. *IEEE Trans. Cybern.* **2021**, *52*, 10721–10734. [CrossRef]
18. Kaveshgar, N.; Huynh, N.; Rahimian, S.K. An efficient genetic algorithm for solving the quay crane scheduling problem. *Expert. Syst. Appl.* **2012**, *39*, 13108–13117. [CrossRef]
19. Kaveshgar, N.; Huynh, N.; Rahimian, S.K. Solving the quay crane scheduling problem using genetic algorithm in MATLAB. In Proceedings of the Trb 91st annual meeting compendium of papers, Transportation Research Board, Washington, DC, USA, 22–26 January 2012; pp. 1–20.
20. Expósito-Izquierdo, C.; Melián-Batista, B.; Moreno-Vega, J.M. An estimation of distribution algorithm for solving the quay crane scheduling problem with availability constraints. *Adv. Knowl.-Based Intell. Inform. Eng. Syst.* **2011**, *243*, 10–19.
21. Daganzo, C. The crane scheduling problem. *Transp. Res. Part B* **1989**, *23*, 159–175. [CrossRef]
22. Sun, D.; Tang, L.; Baldacci, R. A benders decomposition-based framework for solving quay crane scheduling problems. *Eur. J. Oper. Res.* **2019**, *273*, 504–515. [CrossRef]
23. Huang, S.; Li, Y. A bounded two-level dynamic programming algorithm for quay crane scheduling in container terminals. *Comput. Ind. Eng.* **2018**, *123*, 303–313. [CrossRef]
24. Castilla-Rodríguez, I.; Expósito-Izquierdo, C.; Melián-Batista, B.; Aguilar, R.M.; Moreno-Vega, J.M. Simulation-optimization for the management of the transshipment operations at maritime container terminals. *Expert. Syst. Appl.* **2020**, *139*, 112852. [CrossRef]
25. Dik, G.; Kozan, E. A flexible crane scheduling methodology for container terminals. *Flex. Serv. Manuf. J.* **2017**, *29*, 64–96. [CrossRef]
26. Zhen, L.; Hu, H.; Wang, W.; Shi, X.; Ma, C. Cranes scheduling in frame bridges based automated container terminals. *Transp. Res. Part C* **2018**, *97*, 369–384. [CrossRef]
27. Wu, L.; Ma, W. Quay crane scheduling with draft and trim constraints. *Transport. Res. Part E* **2017**, *97*, 38–68. [CrossRef]
28. He, J.L.; Huang, Y.F.; Yan, W.; Wang, S.A. Integrated internal truck, yard crane and quay crane scheduling in a container terminal considering energy consumption. *Expert. Syst. Appl.* **2015**, *42*, 2464–2487. [CrossRef]
29. Hu, Q.M.; Hu, Z.H.; Du, Y.Q. Berth and quay-crane allocation problem considering fuel consumption and emissions from vessels. *Comput. Ind. Eng.* **2014**, *70*, 1–10. [CrossRef]
30. Diabat, A.; Theodorou, E. An integrated quay crane assignment and scheduling problem. *Comput Ind Eng.* **2014**, *73*, 115–123. [CrossRef]
31. He, J.L. Berth allocation and quay crane assignment in a container terminal for the trade-off between time-saving and energy-saving. *Adv. Eng. Inform.* **2016**, *30*, 390–405. [CrossRef]
32. Xin, J.B.; Meng, C.; Ariano, A.; Wang, D.S.; Negenborn, R.R. Mixed-integer nonlinear programming for energy-efficient container handling: Formulation and customized genetic algorithm. *IEEE Trans. Intell. Transp. Syst.* **2021**, *23*, 10542–10555. [CrossRef]
33. He, L.J.; Chiong, R.; Li, W.F.; Budhi, G.S.; Zhang, Y. A multiobjective evolutionary algorithm for achieving energy efficiency in production environments integrated with multiple automated guided vehicles. *Knowl-Based Syst.* **2022**, *243*, 108315. [CrossRef]
34. Zhang, Q.; Li, H. MOEA/D: A multiobjective evolutionary algorithm based on decomposition. *IEEE Trans. Evol. Comput.* **2007**, *11*, 712–731. [CrossRef]
35. Deb, K.; Pratap, A.; Agarwal, S.; Meyarivan, T. A fast and elitist multiobjective genetic algorithm: NSGA-II. *IEEE Trans. Evol. Comput.* **2002**, *6*, 182–197. [CrossRef]
36. Zitzler, E.; Laumanns, M.; Thiele, L. SPEA2: Improving the strength Pareto evolutionary algorithm for multiobjective optimization. In *Evolutionary Methods for Design, Optimization and Control with Applications to Industrial Problems: Proceedings of the EUROGEN2001 Conference, Athens, Greece, 19–21 September 2001*; International Center for Numerical Methods in Engineering (CIMNE): Barcelona, Spain, 2002; Volume 103, pp. 95–100.